



Cite this: *Chem. Sci.*, 2022, **13**, 13264

## Mesoporous ordered films *via* self-assembly: trends and perspectives

Plinio Innocenzi  <sup>ab</sup>

The synthesis of ordered mesoporous films *via* self-assembly represents one of the main accomplishments in nanoscience. In fact, controlling the complex chemical–physical phenomena that govern the process triggered by the solvent's fast evaporation during film deposition has represented a challenging task. Several years after the first articles on the subject, the research in the field entered a new stage. New advanced applications based on the peculiar properties of mesoporous films are envisaged while basic research is still going on, especially to clarify the mechanism behind self-organization in a spatially defined environment and the physics and chemistry in mesoscale porosity. This review has been dedicated to analysing the main trends in the fields and the perspective for future developments.

Received 30th August 2022

Accepted 7th October 2022

DOI: 10.1039/d2sc04828k

[rsc.li/chemical-science](http://rsc.li/chemical-science)

### 1. Introduction

The possibility of fabricating thin films at controlled porosity through self-assembly techniques is one of the fascinating aspects of nanoscience. It is still a frontier research area, even though many years have passed since the first synthesis of mesoporous films in 1994.<sup>1,2</sup> Particularly attractive is the multidisciplinarity of the process in which supramolecular, sol–gel, and colloid chemistry gives the foundation for explaining a complex phenomenon. Research in the field has entered a mature stage where the basic chemical and physical aspects have been well studied, but several issues remain to be explored. Mesoporous films represent a narrow and confined environment of nanoscopic dimensions whose properties are still partially unknown. A better understanding of physics and chemistry in confined nano-scale porous environments would offer new opportunities for advanced functional applications.

This review focus on identifying the recent research trends in the sector that is fast moving.<sup>3,4</sup> It is clear from an analysis of the articles recently published in the scientific literature that research in the field is increasingly focused on the development of specific applications where the possibility of obtaining thin films with controlled porosity in terms of orientation and pore size represents an intrinsic advantage over other types of materials.<sup>5</sup> In particular, the possibility of obtaining films oriented in specific directions with respect to the substrate has undoubtedly represented one of the most interesting results in recent years and has attracted great attention. The pore orientation engineering has paved the way for a whole series of new applications

of mesoporous films. At the same time, the development of nanocomposites using mesoporous films as a matrix represents another challenging frontier. The fabrication of heterostructures based on materials with controlled porosity allows obtaining nanomaterials with unique properties.<sup>6</sup> In particular, the possibility of integrating the new generation nanomaterials, in particular two-dimensional or zero-dimensional nanostructures within mesopores represents an opportunity not to be missed. As far as basic research is concerned, the deposition process of mesoporous thin films has reached a level of understanding now mature, thanks to the numerous studies that have been done previously. However, some aspects remain to be studied and deepened, such as mechanical properties and structure–property correlations in nanocomposites.

In drafting this review, the articles published in the sector in recent years have been considered, which number several hundred, testifying to the great interest that the material and the process still attract. Not all of them have been mentioned, a selection has been necessarily made according to the topics that emerge from the analysis of the literature, also to avoid the review becoming a mere list of articles. The article is restricted to the limited field of mesoporous films that show an organization of the porous phase. It should be underlined that most scientific literature focuses on mesoporous microparticles,<sup>7</sup> the synthesis of which, however, does not take place in the critical conditions dictated by the fast evaporation of the solvent as in films. The review also does not report the fundamentals of the self-assembly process that lead to the formation of structures organized in the mesoscale during evaporation, a process referred to as Evaporation Induced Self-Assembly (EISA). These processes, together with the chemical–physical phenomena that govern them, are well described in numerous excellent reviews<sup>8–12</sup> and books<sup>13</sup> to which the unfamiliar reader in the subject can refer.

<sup>a</sup>Laboratory of Materials Science and Nanotechnology (LMNT), Department of Biomedical Sciences, CR-INSTM, University of Sassari, Viale San Pietro 43/B, Sassari 07100, Italy. E-mail: [plinio@uniss.it](mailto:plinio@uniss.it)

<sup>b</sup>Department of Chemistry, University of United Arab Emirates, Al Ain. United Arab Emirates, United Arab Emirates



## 2. Aligning the mesopores

The most common and historically the first method developed for fabricating mesostructured films is the deposition on a substrate under controlled conditions, typically *via* dip-coating,<sup>14–16</sup> spray coating,<sup>17,18</sup> or spin coating,<sup>19,20</sup> of a starting solution containing all the precursors. The method is relatively simple, and the only requirement is the proper control of the conditions in the deposition chamber, relative humidity, temperature and atmosphere. The self-assembly during the film deposition has been studied in detail and is now well understood. One of the main open issues is the possibility of controlling the orientation of the mesopores using a simple and reliable procedure. In the case of 3D structures that have no preferential orientation, the question is controlling the order on a long range rather than having ordered domains. 2D-hex mesoporous structures, instead, tend to align in a direction parallel to the substrate, with randomly orientated domains.<sup>21</sup> However, many of the most exciting applications require precise pore orientation control with high accessibility from the external environment. In particular, obtaining a perpendicular alignment to the substrate allows for using mesoporous films as advanced sensors and filter membranes. Therefore, much attention has recently been paid to achieve a precise control of the pore orientation and size. Different strategies have been envisaged for such purpose in 2D-hex mesostructures, for instance application of external magnetic fields,<sup>22,23</sup> radio sputtering,<sup>24</sup> controlled fluxes of air,<sup>25</sup> epitaxial growth<sup>26,27</sup> and pre-patterning of the substrate.<sup>28</sup> More recently, alternative methodologies have been developed that have made it possible to open new perspectives using mesoporous films by aligning the mesopores perpendicularly to the substrate.

### 2.1. Seeding block-copolymer layers

In the last years, alternative processes to obtain ordered mesoporous films have been explored. One example is the two-step process based on the deposition of a first surfactant layer followed by a second coating containing the metal oxide precursor (Fig. 1).<sup>29</sup> The method has been applied to obtain

mesoporous  $\text{TiO}_2$  films whose formation is governed by the interdiffusion of the two components, the surfactant and the oxide precursor, at the interface.

The pre-deposition of a block-copolymer template layer has been proven to be a feasible technique for obtaining silica<sup>30</sup> and titania films with tilted and vertically aligned pores with respect to the substrates.<sup>31</sup> The substrate is first immersed in a solution containing a surfactant (Pluronic P123), 1,6-diisocyanatohexane, and a small amount of glycerol used as a cross-linker to stabilize the layer. Onto this layer is deposited *via*-dip-coating the precursor sol with the surfactant, and during the evaporation, vertically aligned mesochannels form.<sup>32,33</sup> The epitaxial alignment of the surfactant hydrophobic blocks induces the orientation across the film. The aligned mesoporous films are particularly stable during calcination at temperatures up to 500 °C, without significant loss of the mesostructured order.<sup>34</sup> Silica thin membranes with uniform and large vertical mesochannels have been also synthesised using a two-step templated growth in solution.<sup>35</sup> At first, the substrate is immersed in a solution containing the surfactant, and then tetraethylorthosilicate (TEOS) in cyclohexane is added drop by drop. Free-standing mesoporous silica membranes have been finally obtained by the poly(methyl methacrylate) (PMMA) assistant transfer method.

### 2.2. Stöber method for the fabrication of vertically oriented mesochannels

Another innovative method has been developed starting from the well-known Stöber process that is used to fabricate silica particles of controlled shape and dimension.<sup>36</sup> The process has been also extended to obtain mesoporous silica particles whose mesochannels are radially oriented towards the surface.<sup>37</sup> The extension of the Stöber process to self-assembled mesoporous films allows for orienting the mesopores perpendicularly to the substrate.<sup>38</sup> The deposition of organized silica films is achieved by immersing the substrate into a Stöber solution that contains the surfactant, cetyltrimethylammonium bromide (CTAB), besides the silica precursor, (TEOS), water, ethanol and ammonia. Mesostructured films with ordered hexagonal

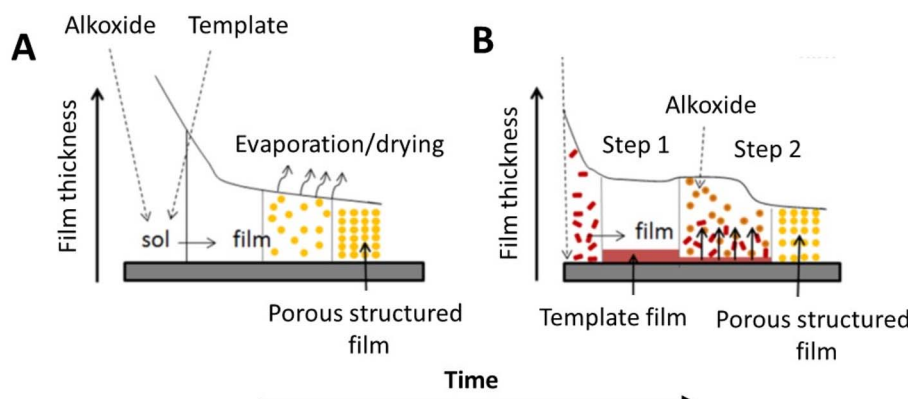


Fig. 1 Comparative pathways of the supported mesoporous film formation by: (A) conventional approach (EISA) using mixtures of precursors (alkoxides) and porogens (surfactants), and (B) alternative procedure using the components in two steps. Modified with permission from ref. 28.



packing of mesochannels perpendicular to the substrate are obtained by immersion in the Stöber solution for a controlled time that allows the spontaneous growth of the silica mesostructure (Fig. 2).

The slow hydrolysis of TEOS in highly basic conditions, with the formation of negatively charged oligomers, favours the electrostatic interaction with the positively charged micelle surface screening at the same time, the micelle–micelle repulsion. In addition, the diffusion of alcohol within the micelles lowers their curvature favouring the transition to cylindrical micelles. In addition, the diffusion of alcohol within the micelles lowers their curvature triggers the transition to cylindrical micelles. Ammonia also plays an important role promoting the hydrogen bonding between the CTAB micelles and the silica oligomers with further decreases of the curvature.

The method has some limitations because a hydrophilic substrate is necessary, and therefore, deposition on silicon is difficult. However, it opens the possibility of preparing membranes with the capability of filtering in the nanoscale. The silica film can be detached from the substrate and used as membranes, and several examples have been reported so far. The synthesis, with small modifications to control the swelling of the micelles during self-assembly, has been employed to obtain mesoporous silica membranes with a uniform thickness of 50 nm, vertical mesopore channels with  $p6mm$  2D-hex symmetry, and pore diameters in the 2.8–11.8 nm range. Self-standing mesoporous silica membranes are obtained *via* polymethylmethacrylate (PMMA) assisted transfer that employs two polyethersulfone layers as the supports. The method has been extensively applied to prepare nano-filters and selective membranes for different applications.<sup>39</sup>

### 2.3. Electrochemically assisted self-assembly (EASA)

An alternative method for the deposition of mesoporous films that has become very popular is the Electrochemically Assisted Self-Assembly (EASA).<sup>40</sup> This technique has been pioneered A. Walcarus and his coworkers<sup>41</sup> and is now a well-established method for the deposition of vertically ordered mesoporous layers on conductive substrates. It has been applied to many applications ranging from electrochromic devices,<sup>42</sup> to label free electrochemical sensors<sup>43</sup> and detection of doxorubicin in human whole blood<sup>44</sup> just to cite some.

The silica sol is initially kept at a pH of around 3–4, a value that makes hydrolysis faster than condensation.<sup>45</sup> The electrochemical process promotes an increase of silica pH at the solution–electrode interface, favouring the polycondensation on the electrode (Fig. 3). At the same time, the applied potential also directs the assembling of a surfactant template layer that, in turn, guides the growth of the mesoporous channels perpendicularly to the electrode. The negatively charged silica clusters that form at pH 9–10 interact at the interface of the transient cationic hemimicelles that form at the interface.<sup>46</sup> The proceed of silica condensation promotes the transformation of the hemicelles into cylindrical micelles forming the template for the vertically aligned mesopores. The mesoporous silica film deposited *via* EASA using CTAB as a cationic surfactant have a pore diameter typically around 2 nm. The pore dimension can be increased by swelling with mesitylene<sup>47</sup> or using surfactants with a longer alkyl chain.<sup>48</sup>

The potentialities of oriented mesochannels in silica films have been further exploited by covalent binding organo-functional species on the pore surface. One example of such applications is a surface modification with electroactive

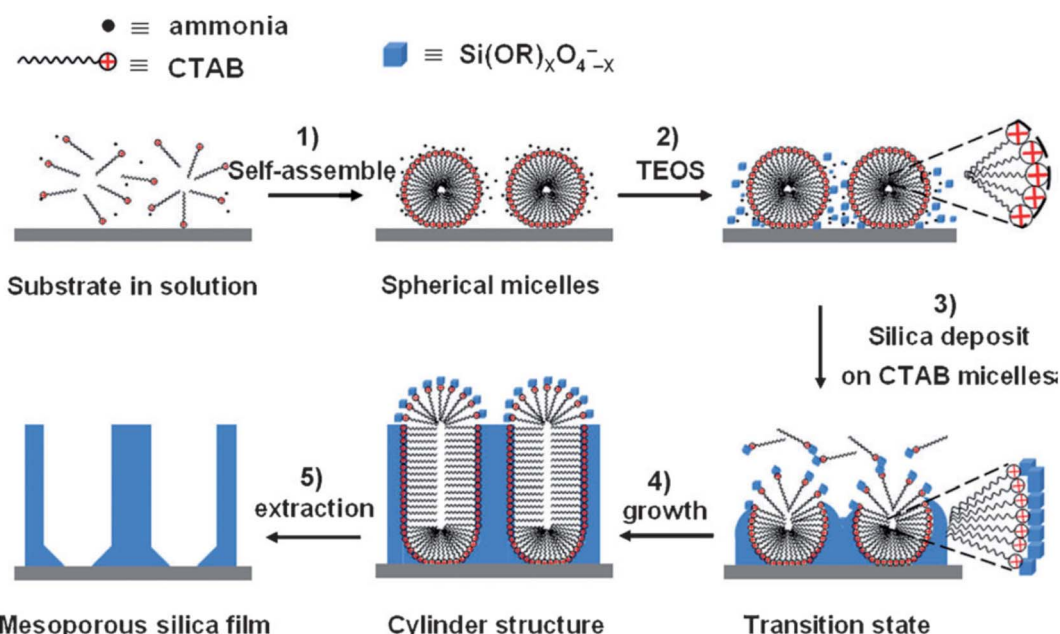


Fig. 2 Formation process of ordered mesoporous silica films with perpendicular mesochannels by the Stöber-solution spontaneous growth procedure. Reproduced with permission from ref. 36.



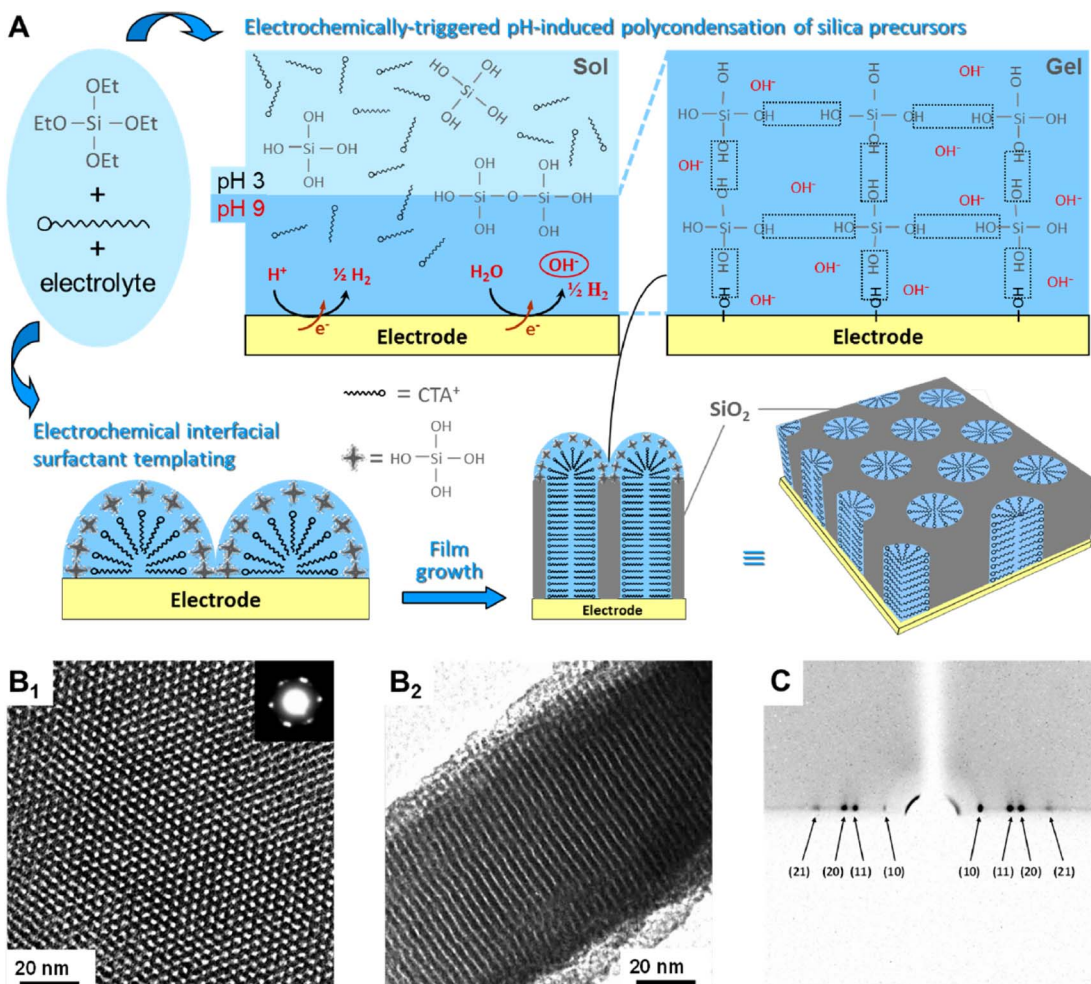


Fig. 3 (A) Schematic illustration of the EASA process. (B) TEM images of the ordered and oriented mesoporous silica film (B<sub>1</sub> top view with electron diffraction pattern as inset; B<sub>2</sub> cross-section). (C) Typical GI-XRD pattern confirming the hexagonal packing of vertically aligned mesopore channels. Reproduced with permission from ref. 40.

molecules, such as ferrocene. It can readily change its redox state *via* electron hopping transfer between adjacent sites, while the charge can propagate over a long distance even in the isolating environment of silica. Interestingly, the attachment on the surface of alkyne and alkene organic groups has been activated *via* click-chemistry.<sup>49</sup> Silica films with vertically oriented channels functionalized by bis(terpyridine) iron(II) have shown an electrochromic response with decolouration from violet within a response time to colouring and bleaching lower than 4 s.<sup>50</sup>

#### 2.4. Orientation by thermally induced film contraction

Phase transformations in mesoporous films are generally observed from drying to annealing stages as a result of the anisotropic stress induced by the shrinkage of the films deposited on a rigid substrate. These phase transformations must be allowed by the selection route. They can also result in a distortion of the pores from spherical to elliptical. Rankin and coworkers have shown an interesting application of these properties.<sup>51</sup> That have fabricated vertically aligned meso-channels with a simple method based on the doping of silica with small amounts of titania (Fig. 4).

Two different doping routes have been employed, dispersion of a small amount of titania (up to 6%) in the silica matrix and fixing of titania at the pore surface by complexation of titanium(IV) isopropoxide with a sugar-based cosurfactant, *n*-dodecyl β-D-maltopyranoside. Both routes produce alignment of the mesopores. Anisotropic stress and annealing of the films trigger the formation of vertically aligned mesopores formed by the merging of randomly oriented pores. The titania “doping” of silica makes the mesostructure more compliant to unidirectional contraction during the thermal shrinkage favouring the coalescence of the pores.

Another example of pore orientation triggered by the thermally induced film contraction is also related to titania mesoporous films.<sup>52</sup> A low molecular weight block copolymer (PS-b-PEO), upon sequential evaporation of ethanol and tetrahydrofuran, form spherical micelles that self-assemble into a body-centered cubic *Im3m* mesostructure. The thermally induced contraction produces vertical channels derived from the coalescence of the pores in the orthogonal interconnected meso-channels (Fig. 5). A similar coalescence process has also been observed in titania films epitaxially grown layer by layer on

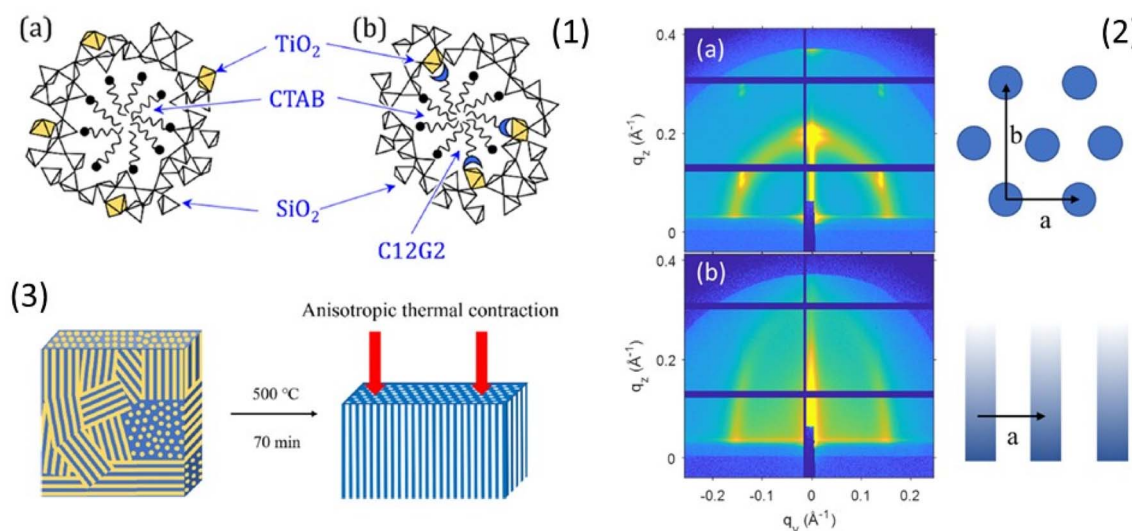


Fig. 4 (1) Schematic showing hypothesized incorporation of Ti (gold polyhedra) (a) throughout pore walls when only CTAB is used as the pore template and (b) at the pore surface due to complexation with dodecyl maltoside. (2) 2D GISAXS pattern of the CTAB-templated silica thin film with 1% titania doping and no sugar surfactant: (a) before calcination, showing a similar *P6mm* structure as undoped silica film with a background of an isotropic ring and (b) after calcination at 500 °C for 70 min. (3) Schematic of the mesopore fusion that transforms the porous structure from randomly oriented pores in titania-doped silica films with no sugar surfactant. Rearranged with permission from ref. 47.

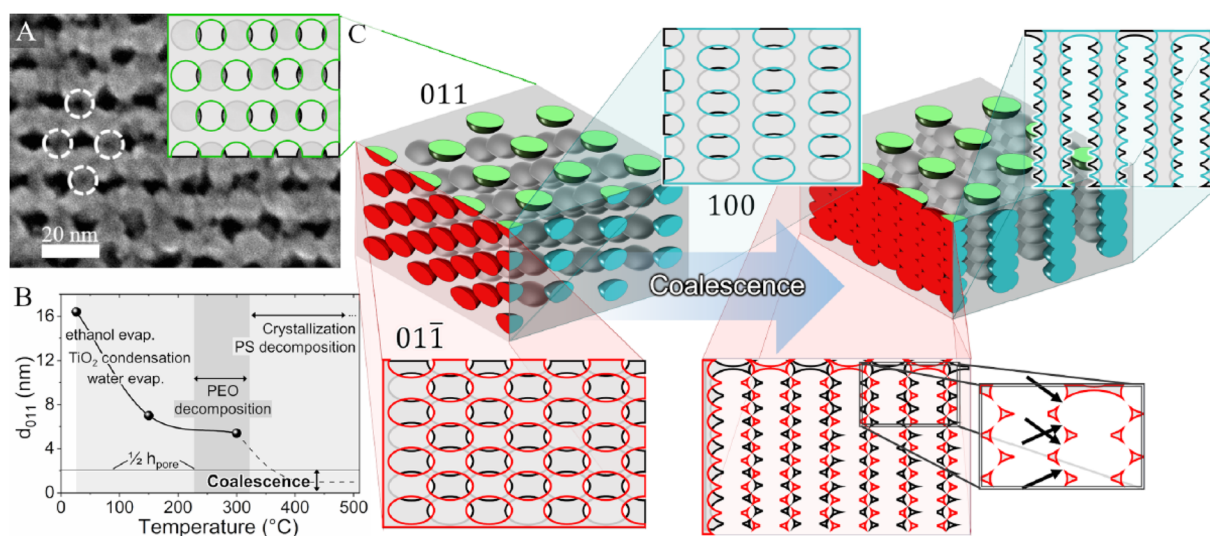


Fig. 5 (A) High-magnification FE-SEM images of mesoporous TiO<sub>2</sub> films. Dashed circles indicate the locations of pores just below the surface. Inset: illustrative view of the bcc structure from the (011) direction. (B) Evolution of the  $d_{011}$ -spacing with temperature. The dotted curve is plotted qualitatively to describe the contraction mechanisms that could not be experimentally observed. The lower horizontal threshold line represents half the pore height ( $1/2h_{\text{pore}}$ , bottom), below which coalescence is expected to occur. (C) Illustration of the 3D pore distribution, along with 2D planar views, before and after coalescence. The side views use colours for the front pores and black/grey for the subsequent plane. The arrows in the lower-right magnified panel represent the possible occurrence of interchannel microporosity originating from the overlapping of neighbouring pores during vertical contraction. Reproduced with permission from ref. 48.

a substrate initially modified by a block copolymer film (Pluronic F127) with a (011)-oriented *Im*<sub>3</sub>*m* cubic mesophase order.<sup>53</sup>

### 3. Understanding and controlling mechanical properties

The mechanical properties of mesoporous films have been the subject of numerous studies mostly focused on measuring

elastic modulus (E) and hardness (H). These properties vary greatly as a function of material structure, such as the degree of crystallinity, porosity, composition, and topology of the mesophase.<sup>54</sup> Various techniques have been employed, such as surface acoustic waves,<sup>55</sup> nanoindentation,<sup>56</sup> ellipsometric porosimetry<sup>57</sup> and X-ray reflectivity<sup>58</sup> to evaluate the mechanical properties in mesoporous films. For a detailed review of the subject, see Soler-Illia and coworkers' work.<sup>59</sup> In general, it has



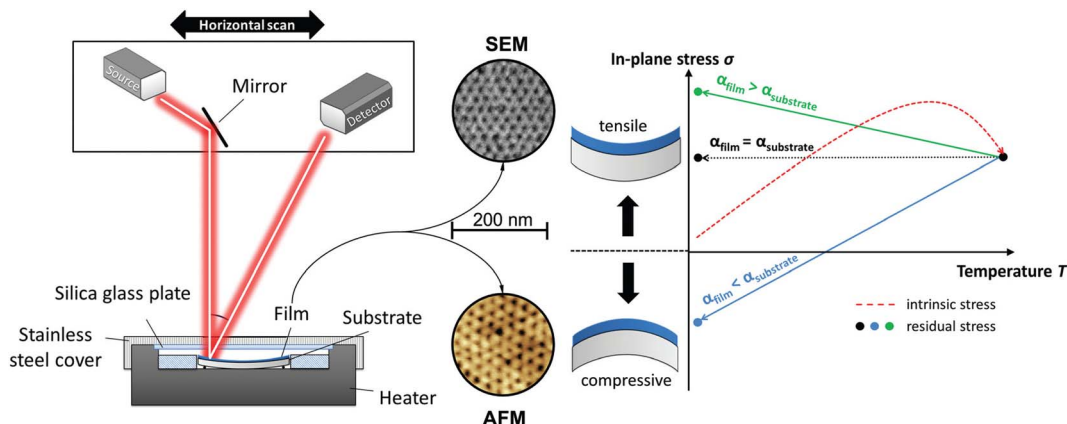


Fig. 6 (Left) Scheme of the setup of the thin film stress instrument used for curvature determination. It has a built-in heater for *in situ* measurements. (Right) Temperature dependence of the in-plane stress while heating (red dotted line) and the following natural cooling process (straight arrows). The different thermal expansion coefficients of the film and substrate directly affect the resulting residual stress. Rearranged with permission from ref. 57.

been found, as expected, a direct relationship between porosity and  $E$  and  $H$ . However, the mechanical properties of thin films deposited by the liquid phase, such as sol-gel and mesoporous films, are highly dependent on the stress generated during heat treatment, which induces shrinkage in the direction perpendicular to the substrate. Such stress can induce fractures and delamination. The shrinkage in the case of mesoporous films can lead to both pore deformation and phase transformations induced precisely by mechanical stress.<sup>60</sup> Kozuka and coworkers<sup>61</sup> have realized a detailed study devoted to understanding the stresses formed in mesoporous films. The mechanical properties of titania and  $\text{Ce}_x\text{Zr}_{1-x}\text{O}_2$  ( $x = 0, 0.5, 1$ ), have been evaluated by the curvature method that measures the

light deflection induced by the concave or convex bending of the films on a substrate (Fig. 6).

The mesoporous films show during the *in situ* process, in comparison to dense sol-gel films, remarkably lower absolute stress values. The block-copolymer template promotes stress relaxation during the process, reflected in a measured smaller intrinsic in-plane stress. The overall residual stress in titania mesoporous films is less than 50% of the one in dense films because the mesopores lower the intrinsic and thermal stress that arise during the heating and cooling stages during film processing.

On the other hand, the stress-strain deformation induced in the mesoporous films can also be used to design the material

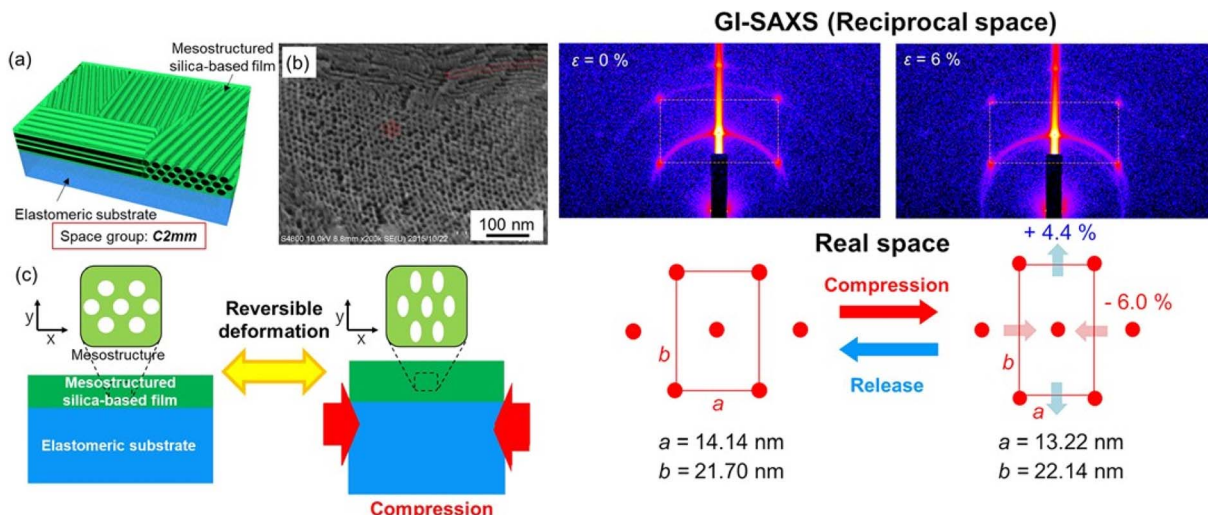


Fig. 7 Left. (a) Schematic illustration of a mesostructured surfactant/silica hybrid film or a mesoporous silica film that has planar rectangular 2D mesostructures with  $C2mm$  symmetry. (b) SEM image of the mesoporous silica film showing a  $C2mm$  mesophase and pores of  $\sim 7$  nm diameter. (c) Concept of the present study: anisotropic and reversible deformation of the mesostructures of the mesostructured silica-based films by compression with accompanying deformation of the elastomeric substrates (PDMS). Right. GI-SAXS images (top) and the corresponding mesostructures (bottom) of the surfactant/silica hybrid film without ( $\varepsilon = 0\%$ ) and with ( $\varepsilon = 6\%$ ) compression (compressive strain  $\varepsilon$  (%),  $dL/L_0 \times 100$ ). Rearranged with permission from ref. 59.

properties as a function of the required application; for instance, the thermoelectric properties of mesoporous ZnO thin films have been found to depend on the stress-strain in the material.<sup>62</sup> Another example is the anisotropic and reversible deformation observed in mesoporous films deposited on elastomeric substrates<sup>63</sup> (Fig. 7). The effect of the mechanically induced stress on the optical properties of a mesoporous silica film has been measured by transferring the film onto an elastomeric poly(dimethylsiloxane) PDMS substrate. The compression of the substrate induced a reversible anisotropic deformation of the mesophase that produced a change in the refractive index.

## 4. Deposition and printing techniques

Developing advanced deposition and printing technologies for mesoporous films is a key issue for integrating the material into functional devices.<sup>64</sup> Several of the applied methods have underlined the high flexibility of film processing; the mesoporous layers can be easily patterned with different processes. The interest is still high and some new methods have been developed. One of these is the slot-die printing that has been successfully applied to deposit mesoporous titania<sup>65,66</sup> and

hematite<sup>67</sup> (Fig. 8) mesostructured films. Slot-die printing is a process that is widely used in the industry for the deposition of liquid solutions on a substrate for large scale manufacturing. Extending the method to mesoporous films is, therefore, important for exploiting the full potentialities of industrial applications.

Another interesting method that has been developed as alternative to dip- and spin-coating for the deposition of mesoporous films is gravure printing (see Fig. 9 for the description of the method).<sup>68</sup>

Gravure printing presents several advantages; ultrathin film of 20 nm can be deposited as a single layer while the film remains highly homogeneous even for small patterns. The film deposited *via* dip-coating can be fabricated with a sufficient quality only on a large substrate because of the rim effects.

Besides innovative fabrication methods, lithography in mesoporous films remains a key issue, especially for applications based on solid-state devices. To fabricate mesoporous silica pillars, lithographic etch masks have been used in combination with inductively coupled plasma (ICP) etching.<sup>69</sup> Large area ordered mesoporous silica nanopillar arrays with smooth vertical sidewall profiles have been fabricated on large areas and different channel depths.

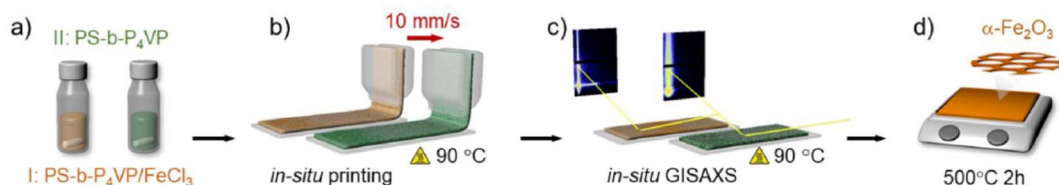


Fig. 8 Fabrication of mesoporous  $\text{Fe}_2\text{O}_3$  films via slot-die coating and high-temperature annealing: (a) PS-*b*-P4VP/FeCl<sub>3</sub> and PS-*b*-P4VP are dissolved in dimethylformamide. (b) Solutions are individually slot-die coated. (c) Film formation of the printed films is followed by *in situ* GISAXS. (d) Slot-die coated PS-*b*-P4VP/FeCl<sub>3</sub> thin film calcined at 500 °C for 2 h to finalize the  $\alpha$ -Fe<sub>2</sub>O<sub>3</sub> thin film. Reproduced with permission from ref. 63.

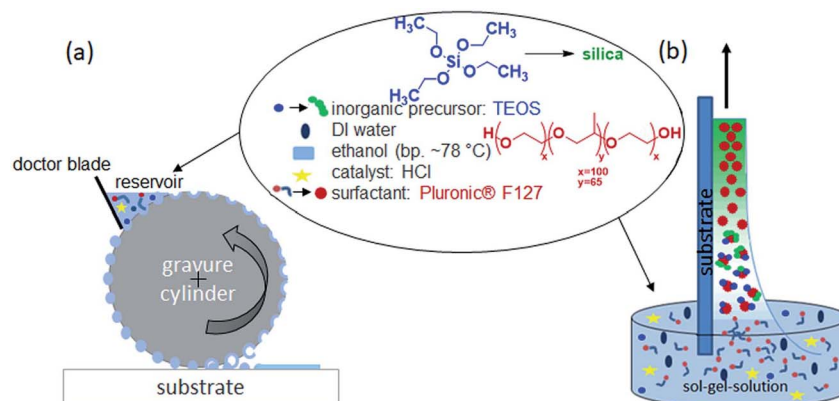


Fig. 9 Comparison of the two mesoporous film preparation strategies, evaporation-induced self-assembly (EISA) by dip-coating or gravure printing. (a) Gravure printing using a metal cylinder transferring the "ink" (sol-gel-solution) to the substrate. The ink is filled out of a reservoir into the cells of the gravure cylinder and directly transferred to the substrate. Excess ink is scraped off by a doctor blade. The cells are not completely emptied, as it comes to a film splitting. The settled fluid spots on the substrate extend to a surface at appropriate ratios of the surface tension of fluid and substrate. The arrangement of the cells specifies the layout to be printed film. The layout repeats after one cylinder revolution. (b) Conventional dip-coating process based on withdrawing a substrate with a defined speed from the sol-gel-solution. The film thickness and quality mainly depends on the used withdrawal speed, solution viscosity and substrate wetting. Reproduced with permission from ref. 64.



Modifying the flat substrate by an array of linear microstructured grooves with a round cross-section has been used to achieve a total in-plane alignment of the mesopores.<sup>70</sup> The mesopores align perpendicularly to the groove long axis driven by the minimization of the elastic energy of the lyotropic liquid crystal phase that results from the self-assembly of the micelles.

Deposition of ordered mesoporous silica into patterned cylinders with pores oriented parallel is another innovative method developed by Hector and coworkers.<sup>71</sup> On a silica on silicon substrate is deposited a TiN layer followed by a second silica film both of which are deposited by sputtering. The silica layer is finally patterned using e-beam lithography and reactive ion etching to fabricate nanoscale pillars with diameters of around 280 nm. The wafer has been then diced into small chips, and mesoporous silica structures have grown in the confined pillar space by drop-casting the EISA solution or *via* dip-coating. Interestingly, the mesopores orient perpendicularly to the pillar surface.

Controlling the thickness is also a critical issue, especially when ultrathin films are required.<sup>72</sup> Wet-etching<sup>73</sup> has been applied to mesoporous silica films by drop-casting an aqueous solution of ammonium fluoride that decreases the film thickness. The interface tension of the solution governs the etching. The same process has also been applied to reduce the thickness of vertically aligned ferrocene-functionalized silica mesoporous films deposited *via* EASA.<sup>74</sup> Furthermore, a post-deposition process using NH<sub>4</sub> has been developed for controlling the porosity in mesoporous silica films.<sup>75</sup> The dissolution process, which proceeds in two well-distinct stages, allows tuning of the film porosity and thickness.

## 5. Negative electrodes and energy storage devices for lithium batteries

One of the areas of mesoporous materials research where researchers' attention has recently been focused is lithium batteries. The use of porosity-controlled materials offers the potential advantage of increased diffusion of the lithium ion while the flexibility of the synthesis method allows for the precise design of different types of devices.<sup>76</sup> Research in this area has focused both on the composition of mesoporous films, particularly silica, titania, lithium titanate, and molybdenum dioxide, but also on pore topology and control of the degree of crystallinity, which is one of the parameters that determines battery effectiveness. Research in the field also includes mesoporous microparticles specifically designed for applications in lithium batteries. Thin-film technology shows a ductility of use that makes it easily integrated into different configurations and types of lithium batteries, and several alternatives have been developed and tested.

MoO<sub>2</sub> mesoporous materials are an example of such application to lithium batteries.<sup>77–79</sup> Ordered mesoporous MoO<sub>2</sub> thin films have been tested to model the correlation between charge storage, crystallinity and porous topology.<sup>80</sup> The thin film configuration allows eliminating carbon additives or binders that can hinder the role of the MoO<sub>2</sub> nanostructure in

modulating the charge storage properties. MoO<sub>2</sub> mesoporous films fired at 600 °C, which is an optimized temperature, can be charged and discharged in 24 h still keeping a Li<sup>+</sup> storage capacity of 158 mA h g<sup>-1</sup>. As the same authors have underlined, the thin film system does not represent a practical energy storage device but allows improving the design of the parameters that control the energy storage in porous materials.

Another material evaluated as an anode for Li-ion microbatteries is nanocrystalline mesoporous of lithium titanate, Li<sub>4</sub>Ti<sub>5</sub>O<sub>12</sub> (LTO), in thin films.<sup>81</sup> LTO anodes potentially have higher stability in charge-discharge cycling, but the disadvantage of reduced electrical conductivity and Li<sup>+</sup> diffusion. On the other hand, LTO as thin films should increase the cation's mobility, overcoming some of the intrinsic limitations of such materials as anode for Li batteries. Nanocrystalline mesoporous carbon-doped Li<sub>4</sub>Ti<sub>5</sub>O<sub>12</sub> thin-film with a pure spinel structure has been obtained *via* self-assembly using an *in situ* synthesis of Li-Ti double alkoxide.

Mesoporous silica films with vertical mesochannels have also been applied to develop anode-free metal lithium batteries<sup>82</sup> that have no excess lithium metal.<sup>83</sup> The absence of the anode increases the battery energy density and avoids dendrite growth, one of the main drawbacks of lithium batteries. Lithium dendrites are metallic microstructures that form on the negative electrode during the charging process. The lack of the anode increases the life cycle and the safe use of the batteries. Mesoporous silica thin layers with vertically oriented mesopores have been used in anode-free devices to improve battery performances and effectively suppress Li dendritic structures (Fig. 10).

The presence of the MSTF regulates the Li<sup>+</sup> flux taking advantage of the ordered spacing between the mesopores, which also contributes to having a uniform Li<sup>+</sup> distribution along in plan structure. Another advantage is the higher

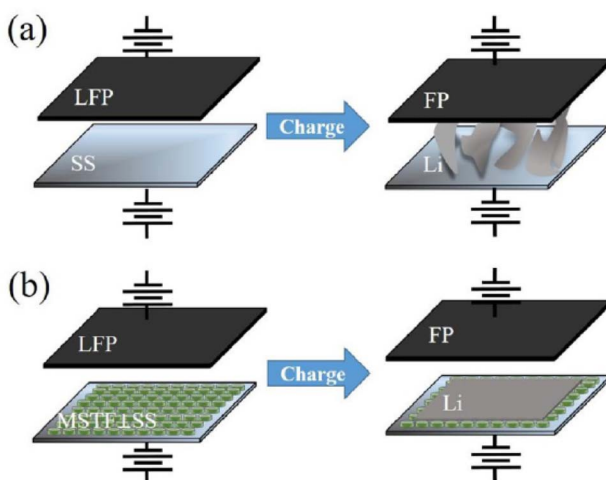
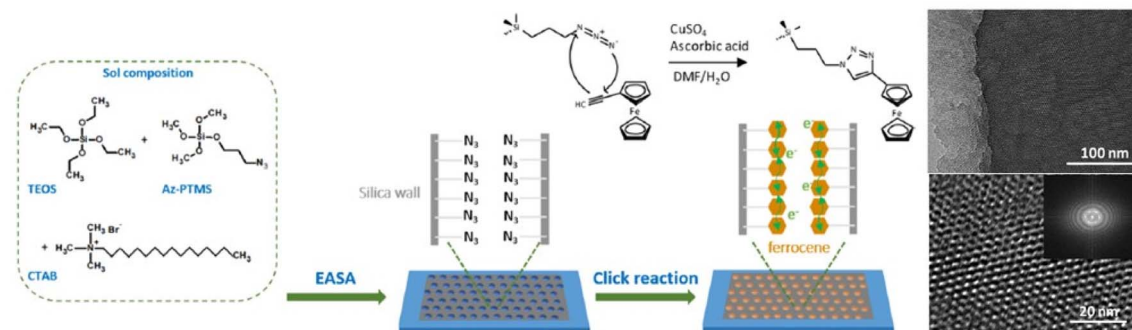


Fig. 10 Schematic illustrations of the Li electrodeposition process on the (a) stainless steel (SS) and (b) mesoporous silica thin films with channels perpendicular to the stainless steel substrate (MSTF  $\perp$  SS) in the anode-free Li metal batteries. Reproduced with permission from ref. 79.





**Fig. 11** Schematic illustration of the preparation process of the ferrocene-functionalized vertically aligned mesoporous silica thin films on a flat ITO electrode. After hydrolysis of the silane precursors, the azide-functionalized silica thin films are further functionalized with ferrocene units by copper-catalyzed azide–alkyne Huisgen reaction (left). Structural characterization of the ferrocene-mesoporous modified with 40% of 3-azidodopropyltrimethoxysilane film. TEM micrographs: top view, cross-sectional view (right top and bottom, respectively). Rearranged with permission from ref. 85.

number of transferred lithium cations into the negatively charged mesochannels that limits the current density and the growth of dendritic structures. In addition, the mesoporous silica matrix is a suitable scaffold for lithium ions and has good wettability with respect to the electrolyte. On the other hand, the limited thickness of the film, around 30 nm, does not significantly enhance the resistance in the battery keeping the conductivity high.

The possibility of modulating the pore organization in terms of dimension, orientation, and pore wall thickness gives mesoporous films enough flexibility to be designed for different device configurations. Mesoporous titania has been widely studied as a material for anode lithium batteries<sup>84</sup> and several examples have also been reported for mesoporous films.<sup>85</sup> In particular, vertically oriented<sup>86</sup> and double diamond structured bicontinuous<sup>87</sup> porous organized structures have been studied for fabricating lithium battery anodes. Porous titania has the advantage with respect to the bulk to increase the  $\text{Li}^+$  ionic and electrical conductivity that is reflected in slow charge–discharge rates. Using the pre-deposition of a block-copolymer layer to vertically align titania mesochannels, films of thickness up to around 1.0  $\mu\text{m}$  and accessible 7–9 nm nanopores have been obtained. A capacity of 254  $\text{mA h g}^{-1}$  is obtained after 200 cycles for a single-layer  $\text{TiO}_2$  film, higher than dense titania films, has been measured. Good performances have also been measured in anodes obtained with bicontinuous titania mesoporous scaffolds with the capacity of 254  $\text{mA h g}^{-1}$  at the current density of 1  $\text{A g}^{-1}$ .

Ordered mesoporous titania films, deposited by spray-coating, have also been fabricated as anode materials in lithium-ion batteries.<sup>88</sup> The material exhibits a high capacity of 680  $\text{mA h g}^{-1}$  at the first discharge, which, however, quickly decreases with the cycles to stabilize at around 170  $\text{mA h g}^{-1}$  after 50 cycles.

A solid-state battery–capacitor based on mesoporous silica films whose walls have been modified by a click chemistry reaction using graphene as the counter electrode has also been prepared<sup>89</sup> (Fig. 11). The device can deliver an energy density of 0.07  $\mu\text{W h cm}^{-2}$  at the high power density of 180  $\mu\text{W cm}^{-2}$ .

Optically transparent thin films with a vertical alignment of the mesopores have been deposited using EASA. The functionalization of the pore surface, to anchor redox-active species, has been done *via* click azide chemistry. This approach allows the introduction of large amounts of organic groups onto the silica walls. The charge propagation occur *via* an electron hopping process between adjacent redox centers.

## 6. Integrating the flatland with mesoporous films, advanced sensing

The integration of two-dimensional materials with a mesoporous matrix, which could be through the formation of a nanocomposite or as an active substrate, is one of the main trends observed in the development of functional applications based on mesoporous films.<sup>90</sup> Graphene, in particular, has been the most used two-dimensional material for this purpose for both applications, but other bidimensional materials, such as BN<sup>91</sup> and  $\text{W}_2\text{S}$ ,<sup>92</sup> have also been considered recently. The development of mesoporous films with pore orientation perpendicular to the substrate, which has now reached an advanced state, has allowed the fabrication of different types of very versatile sensors that use graphene as a conductive substrate. Other graphene materials have been used as an electrode for electrochemical sensing platforms using vertically ordered mesoporous silica (VOMS) channels deposited *via* EISA. Several sensors with fast and highly sensitive responses have been developed using graphene-based architectures. In general, graphene is applied as an electrode on which, using different geometries, are deposited the mesoporous films. One example is the carbendazim (a pesticide) sensor developed using a BN-rGO substrate<sup>93</sup> or the uric acid in serum sensor that employs a 3D macroscopic graphene as substrate.<sup>94</sup>

The ferrocene functionalized silica film coated onto an electro-exfoliated graphene electrode is another example of the integration of graphene with VOMS. The electroactive organically modified mesoporous silicates on graphene oxide-graphite 3D architectures operating *via* electron-hopping for high rate energy storage as pseudo-capacitive material.<sup>95</sup>

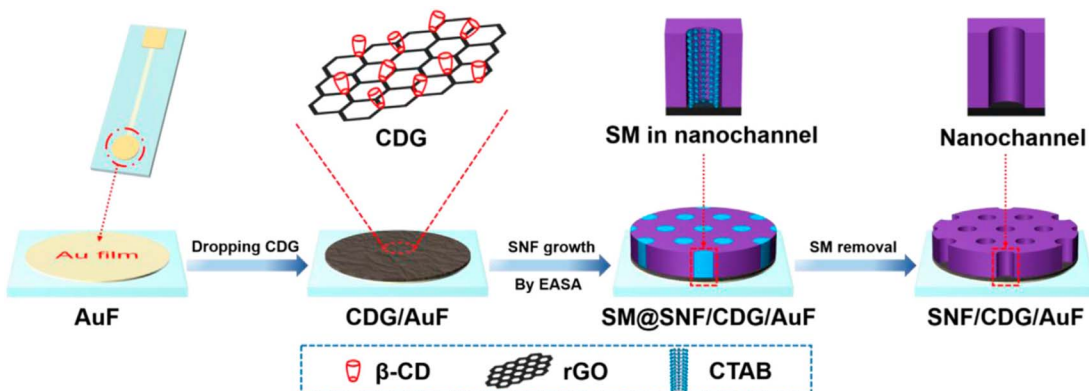


Fig. 12 Illustration of facile preparation of silica nanochannel array film (SNF)/ $\beta$ -cyclodextrin-graphene (CDG)/AuF by EASA method using CDG as nanoadhesive. SM = surfactant micelle. Reproduced with permission from ref. 92.

An example of the different possibilities of designing a device based on the VOMF-graphene architecture is the fabrication is shown in Fig. 12.<sup>96</sup> On a gold substrate is cast a  $\beta$ -cyclodextrin-graphene layer that acts as a functional and conductive layer; the system is a sensor for the electrochemical detection of acetaminophen.

Other examples of mesoporous devices using a graphene layer as an electrode are the sensors for dihydroxybenzene isomers in environmental water samples,<sup>97</sup> for anti-fouling electrochemical detection of tert-butylhydroquinone in cosmetics and edible oils,<sup>98</sup> for the direct electrochemical analysis of human serum,<sup>99</sup> just to cite some.

Mesoporous thin films on graphene field-effect transistors (FETs) have shown the possibility of combining sensing with size-exclusion filtration.<sup>100</sup> The device show a size-excluded electrostatic gating response given by the pore size and a larger amplitude and sensing range compared to bare graphene FETs for charged macromolecules infiltrating the pores.

Incorporating graphene into mesoporous films is not easy because several strict requirements should be fulfilled. For example, graphene must be soluble and well dispersed in the precursor sol, should not disrupt the organization during self-assembly, and the films should remain optically transparent after deposition, which is required for several applications such

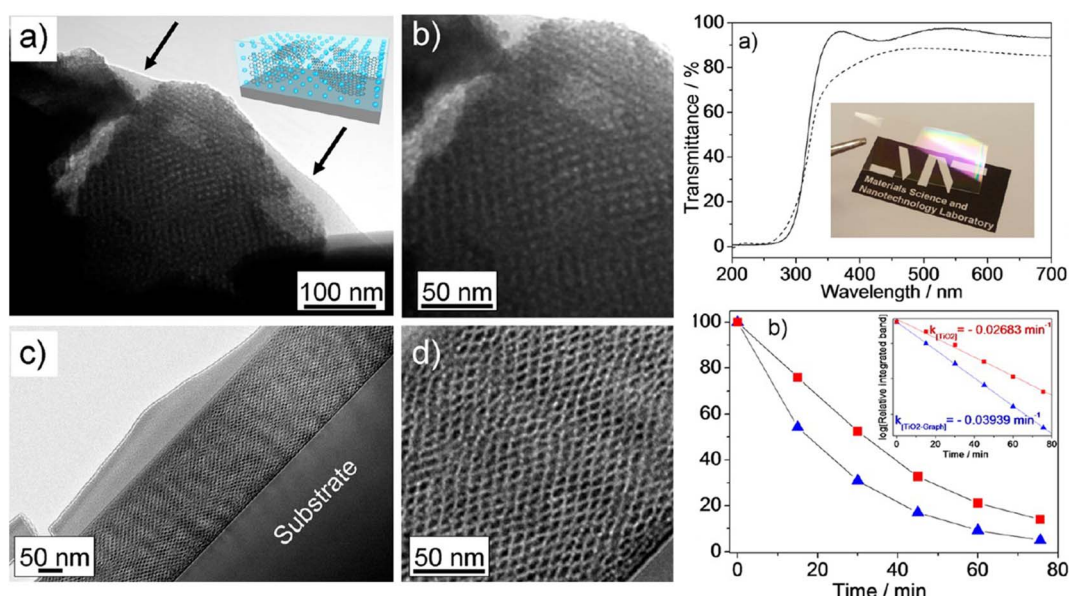


Fig. 13 Left. TEM images of representative areas taken from mesoporous graphene–titania nanocomposite films (2.5 vol% of EG dispersion). (a, b) Film fragments before calcination (thickness  $\approx$  280 nm); arrows indicate the graphene sheets. (c and d) Cross-section dark-field TEM images of the films after calcination. Right. (a) UV-vis spectroscopy of graphene mesoporous nanocomposite films before (solid line) and after (dotted line) thermal calcination (thicknesses  $\approx$  340 and 150 nm, respectively). Inset: picture of the film after thermal treatment. (b) Kinetics of photodegradation of stearic acid deposited on pure titania (red squares) and graphene–titania mesoporous nanocomposites (2.5 vol% of EG dispersion). Inset shows the pseudo-first-order fit of stearic acid decay at increasing time of UV excitation. Reproduced with permission from ref. 97.

as photocatalysis. On the other hand, the incorporation of graphene in titania mesoporous films significantly improves the functional properties and applications in sensing and photocatalysis have been demonstrated. One example is the incorporation of exfoliated graphene into ordered cubic mesoporous films<sup>101</sup> (Fig. 13). The films show an enhanced photocatalytic effect also allowing patterning *via* deep X-ray lithography.

Besides photocatalysis, graphene-titania films have shown a remarkable effect when used as a platform for Surface Enhanced Raman Scattering (SERS).<sup>102</sup> Graphene can enhance the Raman scattering signal through what is indicated as graphene-mediated enhanced Raman scattering (GERS). The enhancement, however, is rather small ( $10\text{--}10^2$ ) because of the chemical mechanism (CM) which governs the charge transfer between graphene and the molecules to detect. This effect is, however, amplified when exfoliated graphene is dispersed in titania mesoporous film giving rise to Ti-GERS (titania-induced graphene-mediated ERS) that has been attributed to synergic interfacial interactions between graphene sheets and titania at the anatase crystallite edges within the nanocomposite.<sup>103</sup> The method to incorporate graphene into mesoporous films is flexible enough to allow fabricating complex heterostructures, for instance, growing inside the mesoporous matrix metal nanoparticles, such as silver<sup>104</sup> and gold.<sup>105</sup> Gold has been thermally reduced *in situ* with preferential nucleation on the surface of the graphene nanosheets.<sup>101</sup> Silver nanoparticles have been instead grown in the graphene-mesoporous titania film by exposition to hard X-rays.<sup>100</sup> Also, in this case, the graphene sheets work as preferential nucleation sites, allowing faster nucleation of the nanoparticles.

Besides graphene, BN<sup>67</sup> and W<sub>2</sub>S<sup>88</sup> nanosheets have also been successfully incorporated *via* one-pot self-assembly into mesoporous ordered titania films. The bidimensional materials can be easily dispersed in the precursor sol and remain homogeneously dispersed into the mesoporous films that keep the organization of the pores. The nanocomposites have been tested for photocatalysis showing improved performances. In the case of BN, the improvement is only observed when defective boron nitride sheets are incorporated in the mesoporous titania films.

Mesoporous films are a feasible matrix not only for graphene sheets but also for graphene<sup>106</sup> and carbon dots.<sup>107–110</sup> An example is the electrochemical sensing platform realized confining graphene quantum dots (GQD) into vertically ordered mesoporous silica channels through electrophoresis.<sup>102</sup> The GQD plays multiple roles by enhancing selectivity as a recognition element and mediator for charge transfer. The integration expects interesting future developments of carbon dots into mesoporous films, which should allow extending the field of application and the construction of functional heterostructures.

## 7. Future outlook

The comprehension of the basic phenomena behind self-assembly in mesoporous ordered films is well established. This is particularly true in the case of silica and titania films,

which are by far the most used and applied in devices and applications. However, despite the previous intense work, some basic knowledge remains to explore. In particular, mesoporous films represent an ideal nanoscale confined environment where the physics and chemistry of reactions and processes are still partly to be explored.

In contrast, research and applications on mesoporous films of different compositions than silica and titania are still quite limited, leaving much room for future investigations. A major trend is the integration of mesoporous films into industrial processes that are effectively applied in terms of scale, cost, material control, environmental impact, and reproducibility. Dip-coating and spin-coating deposition techniques have been the basis for the initial studies of mesoporous films. However, they have severe limitations when they need to be transposed to the market. Therefore, one of the strongest trends is developing sensors based on mesoporous films, mainly using mesostructures oriented vertically to the substrate.

Mesoporous films, when used as sensors, have the advantage that pore wall functionalization can be used to develop highly selective systems. Another area of great interest that is likely to be the subject of intense research in the future is batteries, in which mesoporous films can play an important role. One process that needs to be followed closely is the realization of complex heterostructures based on mesoporous films that may open up new scenarios in sensing and photocatalysis. Integrating two-dimensional materials together with nanoparticles is an example of heterostructures whose development is yet to be explored. Research on mesoporous films after the first phase of studying the basic phenomena governing the self-assembly process has entered a new phase; it is to follow in parallel the development of technologies based on mesoporous films and the innovation proceeding at great speed in nanoscience.

## Author contributions

The author confirms sole responsibility for the contents and preparation of this manuscript.

## Conflicts of interest

There are no conflicts to declare.

## References

- 1 M. Ogawa, Formation of Novel Oriented Transparent Films of Layered Silica-Surfactant Nanocomposites, *J. Am. Chem. Soc.*, 1994, **116**, 7941–7942.
- 2 Y. Lu, R. Ganguli, C. A. Drewien, M. T. Anderson, C. J. Brinker, W. Gong, Y. Guo, H. Soyez, B. Dunn, M. H. Huang and J. I. Zink, Continuous formation of supported cubic and hexagonal mesoporous films by sol-gel dip-coating, *Nature*, 1997, **389**, 364–368.
- 3 K. C.-W. Wu, X. Jiang and Y. Yamauchi, New trend on mesoporous films: precise controls of one-dimensional (1D) mesochannels toward innovative applications, *J. Mater. Chem.*, 2011, **21**, 8934–8939.



4 M. Ogawa, Mesoporous Silica Layer: preparation and Opportunity, *Chem. Rec.*, 2017, **17**, 217–232.

5 P. Innocenzi and L. Malfatti, Mesoporous thin films: properties and applications, *Chem. Soc. Rev.*, 2013, **42**, 4198–4216.

6 P. Innocenzi, L. Malfatti, T. Kidchob and P. Falcaro, Order–Disorder in Self-Assembled Mesostructured Silica Films: A Concepts Review, *Chem. Mater.*, 2009, **21**, 2555–2564.

7 Y. Ren, Z. Ma and P. G. Bruce, Ordered mesoporous metal oxides: synthesis and applications, *Chem. Soc. Rev.*, 2012, **41**, 4909–4927.

8 G. J. A. A. Soler-Illia, P. Vensaus and D. Onna, Chemical methods to produce mesoporous thin films with tunable properties, in *Chemical Solution Synthesis for Materials Design and Thin Film Device Applications*, 2021, ch. 6, pp. 195–229.

9 C. J. Brinker, Y. Lu, A. Sellinger and H. Fan, Evaporation-induced self-assembly: nanostructures made easy, *Adv. Mater.*, 1999, **11**, 579–585.

10 C. Sanchez, C. Boissière, D. Grosso and C. L. L. Nicole, Design, synthesis, and properties of inorganic and hybrid thin films having periodically organized nanoporosity, *Chem. Mater.*, 2008, **20**, 682–737.

11 G. J. A. A. Soler-Illia and P. Innocenzi, Mesoporous Hybrid Thin Films: The Physics and Chemistry Beneath, *Chem. Europ. J.*, 2006, **12**, 4478–4494.

12 D. Grosso, F. Cagnol, G. J. A. A. Soler-Illia, E. L. Crepaldi, H. Amenitsch, A. Brunet-Bruneau, A. Bourgeois and C. Sanchez, Fundamentals of Mesostructuring Through Evaporation-Induced Self-Assembly, *Adv. Funct. Mater.*, 2004, **14**, 309–322.

13 P. Innocenzi, Mesoporous ordered silica films, From Self-Assembly to Order, *Springer series: Advances in Sol-Gel Derived Material and Technologies*, Springer, 2022.

14 D. Grosso, How to exploit the full potential of the dip-coating process to better control film formation, *J. Mater. Chem.*, 2022, **21**, 17033–17038.

15 Y. Lu, R. Ganguli, C. A. Drewien, M. T. Anderson, C. J. Brinker, W. Gong, Y. Guo, H. Soyez, B. Dunn, M. H. Huang and J. I. Zink, *Nature*, 1997, **389**, 364–368.

16 M. Faustini, D. R. Ceratti, B. Louis, M. Boudot, P.-A. Albouy, C. Boissière and D. Grosso, Engineering Functionality Gradients by Dip Coating Process in Acceleration Mode, *ACS Appl. Mater. Interfaces*, 2014, **6**(19), 17102–17110.

17 G. Símonarson, A. Lotsari and A. E. C. Palmqvist, Spray Deposition Synthesis of Locally Ordered Mesoporous Polycrystalline Titania Films at Low Temperature, *Molecules*, 2022, **27**, 303.

18 C. Henrist, C. Toussaint, J. de Vroede, D. Chatzikyriakou, J. Dewalque, P. Colson, A. Maho and R. Cloots, Surfactant-assisted ultrasonic spray pyrolysis of hematite mesoporous thin films, *Microporous Mesoporous Mater.*, 2016, **221**, 182–186.

19 N. Bao, K. Yanagisawa, X. Lu and X. Feng, Spin-coating Preparation of High Quality Mesoporous Titania Nanofilms, *Chem. Lett.*, 2004, **33**, 346–347.

20 J. H. Pana and W. I. Lee, Selective control of cubic and hexagonal mesophases for titania and silica thin films with spin-coating, *New J. Chem.*, 2005, **29**, 841–846.

21 H. Miyata and K. Kuroda, Formation of a continuous mesoporous silica film with fully aligned mesochannels on a glass substrate, *Chem. Mater.*, 2000, **12**, 49–54.

22 Y. Yamauchi, M. Sawada, M. Komatsu, A. Sugiyama, T. Osaka, N. Hirota, Y. Sakka and K. Kuroda, Magnetically Induced Orientation of Mesochannels in Mesoporous Silica Films at 30 Tesla, *Chem.-Asian J.*, 2007, **2**, 1505–1512.

23 Y. Yamauchi, Field-Induced Alignment Controls of One-Dimensional Mesochannels in Mesoporous Materials, *J. Ceram. Soc. Jpn.*, 2013, **121**, 831–840.

24 J. Otomo, S. Wang, H. Takahashi and H. Nagamoto, Microstructure Development of Mesoporous Silica Thin Films with Pore Channels Aligned Perpendicularly to Electrode Surfaces and Application to Proton Conducting Composite Electrolyte Membranes, *J. Membr. Sci.*, 2006, **279**, 256–265.

25 B. Su, X. Lu and Q. Lu, A Facile Method to Prepare Macroscopically Oriented Mesostructured Silica Film: Controlling the Orientation of Mesochannels in Multilayer Films by Air Flow, *J. Am. Chem. Soc.*, 2008, **130**, 14356–14357.

26 E. Richman, T. Brezesinski and S. Tolbert, Vertically Oriented Hexagonal Mesoporous Films Formed through Nanometre-Scale Epitaxy, *Nat. Mater.*, 2008, **7**, 712–717.

27 N. Suzuki, C. Terashima, K. Nakata, K. Katsumata and A. Fujishima, Synthesis of a mesoporous titania thin film with a pseudo-single-crystal framework by liquid-phase epitaxial growth, and enhancement of photocatalytic activity, *RSC Adv.*, 2020, **10**, 40658.

28 H. Miyata and K. Kuroda, Alignment of Mesoporous Silica on a Glass Substrate by a Rubbing Method, *Chem. Mater.*, 1999, **11**, 1609–1614.

29 J. Pérez-Carvajal, P. Aranda, C. Boissière, C. Sanchez and E. Ruiz-Hitzky, Interdiffusive Surfactant Procedure for the Preparation of Nanoarchitected Porous Films: Application to the Growth of Titania Thin Films on Silicon Substrates, *Langmuir*, 2019, **35**, 7169–7174.

30 J. T. Paci, H. B. Man, B. Saha, D. Ho and G. C. Schatz, Synthesis of surfactant-templated silica films with orthogonally aligned hexagonal mesophase, *J. Phys. Chem. C*, 2013, **117**, 17256–17267.

31 V. R. Koganti, D. Dunphy, V. Gowrishankar, M. D. McGehee, X. Li, J. Wang and S. E. Rankin, Generalized Coating Route to Silica and Titania Films with Orthogonally Tilted Cylindrical Nanopore Arrays, *Nano Lett.*, 2006, **6**, 2567–2570.

32 S. j. Nagpure, Q. Zhang, M. Arif Khan, S. Z. Islam, J. Xu, J. Strzalka, Y.-T. Cheng, B. L. Knutson and S. E. Rankin, Layer-by-Layer Synthesis of Thick Mesoporous  $\text{TiO}_2$  Films with Vertically Oriented Accessible Nanopores and Their Application for Lithium-Ion Battery Negative Electrodes, *Adv. Funct. Mater.*, 2018, **28**, 1801849.

33 V. R. Koganti and S. E. Rankin, *J. Phys. Chem. B*, 2005, **109**, 3279–3283.



34 S. Das, S. Nagpure, R. K. Garlapalli, Q. Wu, S. Z. Islam, J. Strzalka and S. E. Rankin, Pore orientation effects on the kinetics of mesostructure loss in surfactant templated titania thin films, *Phys. Chem. Chem. Phys.*, 2016, **18**, 2896–2905.

35 Y. Liu, D. Shen, G. Chen, A. A. Elzatahy, M. Pal, H. Zhu, L. Wu, J. Lin, D. Al-Dahyan, W. Li and D. Zhao, Mesoporous Silica Thin Membranes with Large Vertical Mesochannels for Nanosize-Based Separation, *Adv. Mater.*, 2017, **29**, 1702274.

36 W. Stöber, A. Fink and E. Bohn, Controlled Growth of Monodisperse Silica Spheres in the Micron Size Range, *J. Colloid Interface Sci.*, 1968, **26**, 62–69.

37 M. Grün, I. Lauer and K. K. Unger, The synthesis of micrometer- and submicrometer-size spheres of ordered mesoporous oxide MCM-41, *Adv. Mater.*, 1997, **9**, 254–257.

38 Z. Teng, G. Zheng, Y. Dou, W. Li, C.-Y. Mou, X. Zhang, A. M. Asiri and D. Zhao, Highly Ordered mesoporous Silica Films with Perpendicular Mesochannels by a Simple Stöber-Solution Growth Approach, *Angew. Chem., Int. Ed.*, 2012, **51**, 2173–2177.

39 M.-A. Pizzoccaro-Zilamy, C. Huiskes, E. G. Keim, S. Nicole Sluijter, H. van Veen, A. Nijmeijer, L. Winnubst and M. W. J. Luiten-Olieman, New Generation of Mesoporous Silica Membranes Prepared by a Stöber-Solution Pore-Growth Approach, *ACS Appl. Mater. Interfaces*, 2019, **11**(20), 18528–18539.

40 A. Walcarius, Electroinduced Surfactant Self-Assembly Driven to Vertical Growth of Oriented Mesoporous Films, *Acc. Chem. Res.*, 2021, **54**, 3563–3575.

41 A. Walcarius, Mesoporous Materials and Electrochemistry, *Chem. Soc. Rev.*, 2013, **42**, 4098–4140.

42 S. M. Fonseca, T. Moreira, A. J. Parola, C. Pinheiro and C. A. T. Laia, PEDOT electrodeposition on oriented mesoporous silica templates for electrochromic devices, *Sol. Energy Mater. Sol. Cells*, 2017, **159**, 94–101.

43 W. Argoubi, A. Sanchez, C. Parrado, N. Raouafi and R. Villalonga, Label-free electrochemical aptasensing platform based on mesoporous silica thin film for the detection of prostate specific antigen, *Sens. Actuators, B*, 2018, **255**, 309–315.

44 F. Yan, J. Chen, Q. Jin, H. Zhou, A. Sailjoi, J. Liu and W. Tang, Fast one-step fabrication of a vertically ordered mesoporous silica-nanochannel film on graphene for direct and sensitive detection of doxorubicin in human whole blood, *J. Mater. Chem. C*, 2020, **8**, 7113–7119.

45 P. Innocenzi, *The Sol-to-Gel Transition*, Springer Brief in Materials, 2nd edn, 2019, ISBN: 978-3-030-20029-9.

46 M. Chen, I. Burgess and J. Lipkowski, Potential Controlled Surface Aggregation of Surfactants at Electrode Surfaces - A Molecular View, *Surf. Sci.*, 2009, **603**, 1878–1891.

47 C. Robertson, R. Beanland, S. A. Boden, A. L. Hector, R. J. Kashtiban, J. Sloan, D. C. Smith and A. Walcarius, Ordered Mesoporous Silica Films with Pores Oriented Perpendicular to a Titanium Nitride Substrate, *Phys. Chem. Chem. Phys.*, 2015, **17**, 4763–4770.

48 N. A. N. Mohamed, Y. Han, A. L. Hector, A. R. Houghton, E. Hunter-Sellars, G. Reid, D. R. Williams and W. Zhang, Increasing the Diameter of Vertically Aligned, Hexagonally Ordered Pores in Mesoporous Silica Thin Films, *Langmuir*, 2022, **38**, 2257–2266.

49 N. Vilà, J. Ghanbaja and A. Walcarius, Clickable Bifunctional and Vertically Aligned Mesoporous Silica Films, *Adv. Mater. Interfaces*, 2016, **3**, 1500440.

50 N. Vilà and A. Walcarius, Bis(terpyridine) Iron(II) Functionalized Vertically-Oriented Nanostructured Silica Films: Toward Electrochromic Materials, *Front. Chem.*, 2020, **8**, 830.

51 Y. He, M. A. Khan, A. Drake, R. Ghanim, J. Garay, A. Shirodkar, J. Strzalka, Q. Zhang, B. L. Knutson and S. E. Rankin, Formation of Vertically Oriented Channels during Calcination of Surfactant-Templated Titania-Doped Mesoporous Silica Thin Films, *J. Phys. Chem. C*, 2021, **125**, 22262–22273.

52 V. Malgras, Y. Shirai, T. Takei and Y. Yamauchi, Coalescence-Driven Verticality in Mesoporous  $\text{TiO}_2$  Thin Films with Long-Range Ordering, *J. Am. Chem. Soc.*, 2020, **142**, 15815–15822.

53 M. A. Khan, S. Z. Islam, S. Nagpure, Y. He, N. Wanninayake, R. L. Palmer, J. Strzalka, D. Y. Kim, B. L. Knutson and S. E. Rankin, Epitaxial Formation Mechanism of Multilayer  $\text{TiO}_2$  Films with Ordered Accessible Vertical Nanopores by Evaporation-Driven Assembly, *J. Phys. Chem. C*, 2020, **124**, 1958–1972.

54 E. Barthel, N. Chemin, M. Klotz, V. Rouessac and A. Ayral, Mechanical properties of mesoporous silica thin films: effect of the surfactant removal processes, *Thin Solid Films*, 2006, **495**, 210–213.

55 T. Takimura, N. Hata, S. Takada and T. Yoshino, Determination of mechanical properties of porous silica low- $k$  films on Si substrates using orientation dependence of surface acoustic wave, *Jpn. J. Appl. Phys.*, 2008, **47**, 5400–5403.

56 D. Jauffres, C. Yacou, M. Verdier, R. Dendievel and A. Ayral, Mechanical properties of hierarchical porous silica thin films: experimental characterization by nanoindentation and Finite Element modeling, *Microp. Mesop. Mater.*, 2011, **140**, 120–129.

57 C. Boissiere, D. Grosso, S. Lepoutre, L. Nicole, A. B. Bruneau and C. Sanchez, Porosity and mechanical properties of mesoporous thin films assessed by environmental ellipsometric porosimetry, *Langmuir*, 2005, **21**, 12362–12371.

58 S. Dourdain, D. T. Britton, H. Reichert and A. Gibaud, Determination of the elastic modulus of mesoporous silica thin films by x-ray reflectivity via the capillary condensation of water, *Appl. Phys. Lett.*, 2008, **93**, 183103–183108.

59 D. F. Lionello, J. I. Ramallo, G. J. A. A. Soler-Illia and M. C. Fuertes, Mechanical properties of ordered mesoporous oxides thin films, *J. Sol-Gel Sci. Technol.*, 2022, **101**, 114–139.



60 P. Innocenzi, L. Malfatti, T. Kidchob, P. Falcaro, S. Costacurta, M. Gugliemi, G. Mattei and H. Amenitsch, Thermal induced transitions in self-assembled mesostructured films studied by small angle X-ray scattering, *J. Synchrotron Radiat.*, 2005, **12**, 734–738.

61 P. Cop, S. Kitano, K. Niinuma, B. M. Smarsly and H. Kozuka, In-plane stress development in mesoporous thin films, *Nanoscale*, 2018, **10**, 7002–7015.

62 M.-H. Hong, D. I. Shim, H. H. Cho and H.-H. Park, Effect of mesopore-induced strain/stress on the thermoelectric properties of mesoporous ZnO thin films, *Appl. Surf. Sci.*, 2018, **446**, 160–167.

63 K. Okada, G. Asakura, T. Yamamoto, Y. Tokudome and M. Takahashi, Anisotropic and Reversible Deformation of Mesopores and Mesostructures in Silica-Based films under Mechanical Stimuli toward Adaptive Optical Components, *ACS Appl. Nano Mater.*, 2019, **2**, 2377–2382.

64 P. Innocenzi, T. Kidchob, P. Falcaro and M. Takahashi, Patterning techniques for mesostructured films, *Chem. Mater.*, 2008, **20**, 607–614.

65 N. Li, L. Song, L. Bießmann, S. Xia, W. Ohm, C. J. Brett, E. Hadjixenophontos, G. Schmitz, S. V. Roth and P. Müller-Buschbaum, Morphology Phase Diagram of Slot-Die Printed TiO<sub>2</sub> Films Based on Sol-Gel Synthesis, *Adv. Mater. Interfaces*, 2019, **6**, 1900558.

66 N. Li, W. Chen, L. Song, R. Guo, M. A. Scheel, D. Yang, V. Körstgens, M. Schwartzkopf, S. V. Roth and P. Müller-Buschbaum, In Situ Study of Order Formation in Mesoporous Titania Thin Films Templatized by a Diblock Copolymer during Slot-Die Printing, *ACS Appl. Mater. Interfaces*, 2020, **12**, 57627–57637.

67 S. Yin, T. Tian, C. L. Weindl, K. S. Wienhold, Q. Ji, Y. Cheng, Y. Li, C. M. Papadakis, M. Schwartzkopf, S. V. Roth and P. Müller-Buschbaum, In Situ GISAXS Observation and Large Area Homogeneity Study of Slot-Die Printed PS-b-P4VP and PS-b-P4VP/FeCl<sub>3</sub> Thin Films, *ACS Appl. Mater. Interfaces*, 2022, **14**(2), 3143–3155.

68 N. Herzog, R. Brilmayer, M. Stanzel, A. Kalyta, D. Spiehl, E. Dörsam, C. Hess and A. Andrieu-Brunsen, Gravure printing for mesoporous film preparation, *RSC Adv.*, 2019, **9**, 23570–23578.

69 T. Ghoshal, A. Thorat, N. Prochukhan and M. A. Morris, Fabrication of Dimensional and Structural Controlled Open Pore, Mesoporous Silica Topographies on a Substrate, *Nanomater.*, 2022, **12**, 2223.

70 H. Miyata and M. Takahashi, Lithographically Formed Fine Wavy Surface Morphology for Universal Alignment Control of Mesochannels in Mesostructured Silica Films, *Langmuir*, 2021, **37**, 2179–2186.

71 S. Soule, G. E. Moehl, R. Huang, Y. J. Noori, K. S. Kiang, C. H. Kees de Groot, R. Beanland, D. C. Smith and A. L. Hector, Confining the growth of mesoporous silica films into nanospaces: towards surface nanopatterning, *Nanoscale Adv.*, 2022, **4**, 1105–1111.

72 M. Kobayashi, K. Susuki, T. Otani, S. Enomoto, H. Otsuji, Y. Kuroda, H. Wada, A. Shimojima, T. Homma and K. Kuroda, Thickness control of 3-dimensional mesoporous silica ultrathin films by wet-etching, *Nanoscale*, 2017, **9**, 8321–8329.

73 Y. Minhao, M. J. Henderson and A. Gibaud, On the Etching of Silica and Mesoporous Silica Films Determined by X-Ray Reflectivity and Atomic Force Microscopy, *Thin Solid Films*, 2009, **517**, 3028–3035.

74 T. Sikolenko, C. Despas and A. Walcarus, Thickness control in electrogenerated mesoporous silica films by wet etching and electrochemical monitoring of the process, *Electrochim. Commun.*, 2019, **100**, 11–15.

75 J. Loizillon, M. Putero and D. Grossi, Tuning Mesoporous Silica Film Accessibility Through Controlled Dissolution in NH<sub>4</sub>F: Investigation of Structural Change by Ellipsometry Porosimetry and X-ray Reflectivity, *J. Phys. Chem. C*, 2019, **123**, 30398–30406.

76 G. O. Park, J. Yoon, S. B. Park, Z. Li, Y. S. Choi, W. S. Yoon, H. Kim and J. M. Kim, Nanostructural uniformity of ordered mesoporous materials: governing lithium storage behaviors, *Small*, 2018, **14**, 1702985.

77 J. K. Shon, H. S. Lee, G. O. Park, J. Yoon, E. Park, G. S. Park, S. S. Kong, M. Jin, J. M. Choi, H. Chang, S. Doo, J. M. Kim, W. S. Yoon, C. Pak, H. Kim and G. D. Stucky, Discovery of abnormal lithium-storage sites in molybdenum dioxide electrodes, *Nat. Commun.*, 2016, **7**, 1–9.

78 Y. Shi, B. Guo, S. a. Corr, Q. Shi, Y.-S. Hu, K. R. Heier, L. Chen, R. Seshadri and G. D. Stucky, Ordered mesoporous metallic MoO<sub>2</sub> materials with highly reversible lithium storage capacity, *Nano Lett.*, 2009, **9**, 4215–4220.

79 X. Fang, B. Guo, Y. Shi, B. Li, C. Hua, C. Yao, Y. Zhang, Y. S. Hu, Z. Wang, G. D. Stucky and L. Chen, Enhanced Li storage performance of ordered mesoporous MoO<sub>2</sub> via tungsten doping, *Nanoscale*, 2012, **4**, 1541–1544.

80 Y. Yan, H.-S. Kim, J. B. Cook, S. Robbennolt, B. Dunn and S. H. Tolbert, Mesoporous MoO<sub>2</sub> thin films for high rate Li<sup>+</sup> storage: effect of crystallinity and porous structure, *Solid State Sciences*, 2022, **129**, 106890.

81 J. Mosa and M. Aparicio, Sol-Gel Synthesis of Nanocrystalline Mesoporous Li<sub>4</sub>Ti<sub>5</sub>O<sub>12</sub> Thin-Films as Anodes for Li-Ion Microbatteries, *Nanomaterials*, 2020, **10**, 1369.

82 J. Qian, B. D. Adams, J. Zheng, W. Xu, W. A. Henderson, J. Wang, M. E. Bowden, S. Xu, J. Hu and J. G. Zhang, Anode-Free Rechargeable Lithium Metal Batteries, *Adv. Funct. Mater.*, 2016, **26**, 7094–7102.

83 C.-A. Lo, C.-C. Chang, Y.-W. Tsai, S.-K. Jiang, B. J. Hwang, C.-Y. Mou and H.-L. Wu, Regulated Li Electrodeposition Behavior through Mesoporous Silica Thin Film in Anode-Free Lithium Metal Batteries, *ACS Appl. Energy Mater.*, 2021, **4**, 5132–5142.

84 M. G. Fischer, X. Hua, B. D. Wilts, I. Gunkel, T. M. Bennett and U. Steiner, Mesoporous Titania Microspheres with Highly Tunable Pores as an Anode Material for Lithium Ion Batteries, *ACS Appl. Mater. Interfaces*, 2017, **9**(27), 22388–22397.

85 O. F. McRae, Q. Xia, S. Tjaberings, A. H. Gröschel, C. D. Ling and M. Müllner, Block copolymer-directed synthesis of



porous anatase for lithium-ion battery electrodes, *J. Polym. Sci., Part A-1: Polym. Chem.*, 2019, **57**, 1890–1896.

86 S. Nagpure, Q. Zhang, M. A. Khan, S. Z. Islam, J. Xu, J. Strzalka, Y. T. Cheng, B. L. Knutson and S. E. Rankin, Layer-by-layer synthesis of thick mesoporous  $\text{TiO}_2$  films with vertically oriented accessible nanopores and their application for lithium-ion battery negative electrodes, *Adv. Funct. Mater.*, 2018, **28**, 1801849.

87 Q. Sheng, Q. Li, L. Xiang, T. Huang, Y. Mai and L. Han, Double diamond structured bicontinuous mesoporous titania templated by a block copolymer for anode material of lithium-ion battery, *Nano Res.*, 2021, **14**, 992–997.

88 G. Simonarson, G. Calcagno, A. Lotsari and A. E. C. Palmqvist, Electrochemical and structural characterization of lithiation in spray deposited ordered mesoporous titania as an anode for Li ion batteries, *RSC Adv.*, 2020, **10**, 20279–20287.

89 J. Wang, N. Vilà and A. Walcarus, Redox-Active Vertically Aligned Mesoporous Silica Thin Films as Transparent Surfaces for Energy Storage Applications, *ACS Appl. Mater. Interfaces*, 2020, **12**, 24262–24270.

90 P. Innocenzi, L. Malfatti and D. Carboni, Graphene and carbon nanodots in mesoporous materials: an interactive platform for functional applications, *Nanoscale*, 2015, **7**, 12759–12772.

91 J. Ren, L. Stagi, L. Malfatti, S. Garroni, S. Enzo and P. Innocenzi, Boron Nitride-Titania Mesoporous Film Heterostructures, *Langmuir*, 2021, **37**, 5348–5355.

92 J. Ren, L. Stagi, L. Malfatti, V. Paolucci, C. Cantalini, S. Garroni, M. Mureddu and P. Innocenzi, Improving the photocatalytic activity of mesoporous titania films through the formation of  $\text{WS}_2/\text{TiO}_2$  nano-heterostructures, *Nanomaterials*, 2022, **12**, 1074.

93 Y. Zou, X. Zhou, L. Xie, H. Tang and F. Yan, Vertically-Ordered Mesoporous Silica Films Grown on Boron Nitride-Graphene Composite Modified Electrodes for Rapid and Sensitive Detection of Carbendazim in Real Samples, *Front. Chem.*, 2022, **10**, 939510.

94 X. Zhu, L. Xuan, J. Gong, J. Liu, X. Wang, F. Xi and J. Chen, Three-dimensional macroscopic graphene supported vertically-ordered mesoporous silica-nanochannel film for direct and ultrasensitive detection of uric acid in serum, *Talanta*, 2022, **238**, 123027.

95 J. Wang, N. Vilà and A. Walcarus, Electroactive Organically Modified Mesoporous Silicates on Graphene Oxide-Graphite 3D Architectures Operating with Electron-Hopping for High Rate Energy Storage, *Electrochim. Acta*, 2021, **366**, 137407.

96 H. Zhou, Y. Ding, R. Su, D. Lu, H. Tang and F. Xi, Silica Nanochannel Array Film Supported by  $\beta$ -Cyclodextrin-Functionalized Graphene Modified Gold Film Electrode for Sensitive and Direct Electroanalysis of Acetaminophen, *Front. Chem.*, 2022, **9**, 812086.

97 F. Yan, T. Luo, Q. Jin, H. Zhou, A. Sailjoi, G. Dong, J. Liu and W. Tang, Tailoring molecular permeability of vertically-ordered mesoporous silica-nanochannel films on graphene for selectively enhanced determination of dihydroxybenzene isomers in environmental water samples, *J. Hazard. Mater.*, 2021, **410**, 124636.

98 F. Yan, M. Wang, Q. Jin, H. Zhou, L. Xie, H. Tang and J. Liu, Vertically-ordered mesoporous silica films on graphene for anti-fouling electrochemical detection of tert-butylhydroquinone in cosmetics and edible oils, *J. Electroanal. Chem.*, 2021, **881**, 114969.

99 F. Xi, L. Xuan, L. Lu, J. Huang, F. Yan, J. Liu, X. Dong and P. Chen, Improved adhesion and performance of vertically-aligned mesoporous silica-nanochannel film on reduced graphene oxide for direct electrochemical analysis of human serum, *Sens. Actuators, B*, 2019, **288**, 133–140.

100 S. Alberti, E. Piccinini, P. G. Ramirez, G. S. Longo, M. Ceolín and O. Azzaroni, Mesoporous thin films on graphene FETs: nanofiltered, amplified and extended field-effect sensing, *Nanoscale*, 2021, **13**, 19098–19108.

101 L. Malfatti, P. Falcaro, A. Pinna, B. Lasio, M. F. Casula, D. Loche, A. Falqui, B. Marmiroli, H. Amenitsch, R. Sanna, A. Mariani and P. Innocenzi, Exfoliated Graphene into Highly Ordered Mesoporous Titania Films: Highly Performing Nanocomposites from Integrated Processing, *ACS Appl. Mater. Interfaces*, 2014, **6**, 795–802.

102 L. Malfatti, P. Falcaro, B. Marmiroli, H. Amenitsch, M. Piccinini, A. Falqui and P. Innocenzi, Nanocomposite Mesoporous Ordered Films for Lab-On-Chip Intrinsic Surface Enhanced Raman Scattering Detection, *Nanoscale*, 2011, **3**, 3760–3766.

103 D. Carboni, B. Lasio, D. Loche, M. F. Casula, A. Mariani, L. Malfatti and P. Innocenzi, Introducing Ti-GERS: Raman Scattering Enhancement in Graphene-Mesoporous Titania Films, *J. Phys. Chem. Lett.*, 2015, **6**, 3149–3154.

104 L. Malfatti, D. Carboni, A. Pinna, B. Lasio, B. Marmiroli and P. Innocenzi, *In situ* growth of Ag nanoparticles in graphene- $\text{TiO}_2$  mesoporous films induced by hard X-ray, *J. Sol-Gel Sci. Technol.*, 2016, **79**, 295–302.

105 D. Carboni, B. Lasio, V. Alzari, A. Mariani, D. Loche, M. F. Casula, L. Malfatti and P. Innocenzi, Graphene-mediated surface enhanced Raman scattering in silica mesoporous nanocomposite films, *Phys. Chem. Chem. Phys.*, 2014, **16**, 25809–25818.

106 L. Lu, L. Zhou, J. Chen, F. Yan, J. Liu, X. Dong, F. Xi and P. Chen, Nanochannel-Confined Graphene Quantum Dots for Ultrasensitive Electrochemical Analysis of Complex Samples, *ACS Nano*, 2018, **12**, 12673–12681.

107 A. Vassilakopoulou, V. Georgakilas, N. Vainos and I. Koutselas, Successful entrapment of carbon dots within flexible free-standing transparent mesoporous organic-inorganic silica hybrid films for photonic applications, *J. Phys. Chem. Solids*, 2017, **103**, 190–196.

108 K. Suzuki, L. Malfatti, D. Carboni, D. Loche, M. Casula, A. Moretto, M. Maggini, M. Takahashi and P. Innocenzi, Energy Transfer Induced by Carbon Quantum Dots in Porous Zinc Oxide Nanocomposite Films, *Phys. Chem. C*, 2015, **119**, 2837–2843.

109 C. M. Carbonaro, D. Chiriu, L. Stagi, M. F. Casula, S. V. Thakkar, L. Malfatti, K. Suzuki, P. C. Ricci and



R. Corpino, Carbon Dots in Water and Mesoporous Matrix: Chasing the Origin of their Photoluminescence, *J. Phys. Chem. C*, 2018, **122**, 25638–25650.

110 C. M. Carbonaro, S. V. Thakkar, R. Ludmerczki, C. Olla, A. Pinna, D. Loche, L. Malfatti, F. C. Marincola and

M. F. Casula, How porosity affects the emission of fluorescent carbon dot-silica porous composites, *Microporous Mesoporous Mater.*, 2020, **305**, 110302.

